Research article

Journal of MASS SPECTROMETRY

Received: 30 April 2012 Revised: 22 June 2012 Accepted: 8 July 2012 Published online in Wiley Online Library

(wileyonlinelibrary.com) DOI 10.1002/jms.3063

Study of the fragmentation of arginine isobutyl ester applied to arginine quantification in *Aedes aegypti* mosquito excreta

David R. Bush, Vicki H. Wysocki and Patricia Y. Scaraffia*

It has been demonstrated that argininolysis and uricolysis are involved in the synthesis and excretion of urea in *Aedes aegypti* female mosquitoes. To further investigate the metabolic regulation of urea in female mosquitoes, it is desirable to have a rapid and efficient method to monitor arginine (Arg) concentration in mosquito excreta. Thus, a procedure currently used for the identification of Arg in urea cycle disorders in newborn babies was adapted to analyze Arg in *A. aegypti* excreta. The fragmentation patterns of the isobutyl esters of Arg and $^{15}N_2$-Arg (labeled at the guanidino group) were explored by electrospray ionization (ESI)-tandem mass spectrometry and fragmentation pathways not described before were characterized. In addition, Arg, $^{18}O_2$-Arg, $^{15}N_2$-Arg and $^{15}N_2$-$^{18}O_2$-Arg were also analyzed to elucidate some of the minor fragments in greater detail. Mosquito excreta from individual females were collected before and at different times after feeding a blood meal, mixed with $^{15}N_2$-Arg, an internal standard, and then derivatized as isobutyl esters. Based on the fragmentation mechanisms of Arg standards, studied by MS^2 and MS^3, Arg in the mosquito excreta was successfully analyzed by ESI-multiple reaction monitoring in a triple-quadrupole mass spectrometer. Arg excretion was monitored over a 120 h window before and after feeding female mosquitoes with a blood meal, with the maximum level of Arg excretion observed at 36–48 h post blood feeding. This method provides an efficient and rapid tool to quantify Arg in individual blood-fed mosquitoes, and can be applied to other organisms, whose small size severally limits the use of conventional biochemical analysis. Copyright © 2012 John Wiley & Sons, Ltd.

Supporting information may be found in the online version of this article.

Keywords: electrospray ionization-MS; isobutyl ester of arginine; multiple reaction monitoring; amino acid analysis; *Aedes aegypti* mosquitoes

Introduction

Millions of people worldwide are annually infected by etiological agents that are transmitted by mosquitoes.[1–3] To combat this serious health problem, new strategies need to be developed. A better understanding of metabolic processes that occur in these hematophagous insects could lead to the discovery of specific targets able to block or disrupt one or more critical metabolic pathways causing a significant reduction in the mosquito populations and the diseases they transmit.

Anautogenous mosquitoes, such as *Aedes aegypti*, require a blood meal to obtain the nutrients and complete oogenesis. During blood digestion, most of the amino acids are deaminated resulting in the release of ammonia, a toxic compound. In spite of the massive deamination that occurs, *A. aegypti* females detoxify ammonia and eliminate the nitrogen excess very efficiently.[4,5] To better understand the biochemical mechanisms involved in this critical metabolic process, we have used an infusion-based multiple reaction monitoring (MRM) technique.[6–10] Thus, ammonia metabolism in *A. aegytpi* mosquitoes has been successfully studied in whole body, excreta and specific tissues of *A. aegypi* females, the main vectors of dengue and yellow fever.[7–9] We have observed that ammonia metabolism takes place in three phases: fixation, assimilation and excretion. The fixation and assimilation phases are mainly mediated by the glutamine synthetase/glutamate synthase (GS/GltS) pathway. However, pyrroline-5-carboxylate synthase, pyrroline-5-carboxylate reductase, glutamate dehydrogenase, alanine aminotransferase are also active during these phases.[7,9] In the excretion phase, several nitrogen compounds, such as uric acid, ammonia, urea, amino acids, hematin,[11] allantoin and allantoic acid,[8] are eliminated. Surprisingly, the urea synthesis in mosquitoes is generated by two different metabolic pathways called argininolysis[11] and uricolysis.[8] The argininolysis is catalyzed by arginase, whereas the uricolysis is catalyzed by urate oxidase, allantoinase and allantoicase.[8] In contrast to vertebrates, mosquitoes lack the urea cycle because they do not have the gene encoding ornithine transcarbamylase, also called ornithine carbamoyltransferase.[12] This makes arginine (Arg) an essential amino acid for mosquitoes. The action of the arginase in mosquitoes is limited to Arg from diet or from endogenous protein turnover. Since both argininolysis and uricolysis contribute to the urea pool, we are interested in uncovering the mechanisms involved in the metabolic regulation of urea in mosquitoes. To reach this goal, first it is necessary to have a rapid and efficient method to monitor Arg concentration in mosquito excreta.

Electrospray ionization (ESI)-MRM is a traditional tandem mass spectrometry technique for selectively and sensitively quantifying small molecules and metabolites,[13,14] as well as proteins.[15,16] The technique is currently used in clinical mass spectrometry to

* *Correspondence to: Patricia Y. Scaraffia, Department of Chemistry and Biochemistry, The University of Arizona, Tucson, AZ 85721–0088, Phone: (520) 626–5052, Fax: (520) 626–9204. Email: scaraffi@email.arizona.edu*

Department of Chemistry and Biochemistry, The University of Arizona, Tucson, AZ, 85721, United States

Journal of MASS SPECTROMETRY

detect amino acid disorders in newborns.[17–24] Dried blood spots extracted from newborn babies are commonly derivatized to their n-butyl esters and identified by MRM. Arg is one of the amino acids monitored by this method for the detection of inherited errors of the urea cycle such as argininosuccinic aciduria[17] and arginemia.[19]

In the present study, we applied the aforementioned MRM method to detect Arg[17–20] by using isobutanol, instead of n-butanol, to derivatize Arg to its isobutyl ester because it has been reported that the isobutyl ester derivative enhances ionization efficiencies compared to the n-butyl ester derivative.[25] Although Arg fragmentation mechanisms have been studied in significant detail and many of the major fragmentation pathways have been elucidated using α-^{15}N labeling and computational modeling,[26–30] the isobutyl ester fragmentation mechanisms have not been described. Therefore, in this report, we studied the fragmentation pathway of the isobutyl ester of Arg and $^{15}N_2$-Arg (labeled at guanidino group). Because the fragmentation pathway of Arg parallels that of the isobutyl ester, $^{18}O_2$-Arg, $^{15}N_2$-Arg and $^{15}N_2$-$^{18}O_2$-Arg were also studied to elucidate some of the minor fragments in greater detail. Based on the fragmentation mechanism of Arg standards analyzed by MS/MS, Arg in *A. aegypti* excreta was successfully monitored by MRM using two different transitions. Excreta obtained from individual mosquitoes were mixed with $^{15}N_2$-Arg as an internal standard and derivatized as isobutyl esters. Arg excretion was monitored during a time course of 120 h before and after feeding female mosquitoes with a blood meal.

Experimental section

Reagents

The labeled isotope $^{15}N_2$-Arg (labeled at the guanidino group) was purchased from Cambridge Isotopes Laboratories (Andover, MA, USA). Unlabeled Arg, ^{18}O-water, isobutanol, sucrose and ATP were obtained from Sigma-Aldrich (St. Louis, MO, USA). Methanol and acetic acid were purchased from EMD Chemicals, Inc. (Gibbstown, NJ, USA). All the solvents were of analytical or high-performance liquid chromatography grade. Bovine blood meal was purchased from Pel-Freez Biologicals (Rogers, AR, USA). Isobutanol/3M hydrogen chloride was prepared by slowly adding acetyl chloride to cold isobutanol (1:4 v/v) under anhydrous conditions purged with N_2.

Arginine derivatization

In order to move the analyte to a higher *m/z* range away from a noisy low *m/z* region, and to increase fragmentation efficiency, unlabeled Arg and labeled $^{15}N_2$-Arg standards were derivatized to their isobutyl esters by using the procedure previously described for other amino acids.[6–8] Briefly, 2.5 μL of 1 mM Arg or $^{15}N_2$-Arg was dried using a vacuum centrifuge. The residue was treated with 200 μL of isobutanol/3M HCl at room temperature for 50 min, and the excess reagent was removed under a stream of N_2.

Labeling of arginine by exchange with ^{18}O-water

Arg and $^{15}N_2$-Arg were completely labeled with ^{18}O at the carboxylic acid by a method previously reported.[31] Briefly, 3 mg of each amino acid was dissolved in 920 μL of ^{18}O-water, followed by 80 μL of 12 M HCl. The samples were heated at 70°C for 72 h. In order to minimize back-exchange of ^{18}O, the samples were aliquoted, dried in a vacuum centrifuge and reconstituted only prior to use.

Mosquito excreta preparation for mass spectrometry analysis

A. aegypti mosquitoes (NIH-Rockefeller strain) were reared under standard conditions.[4] Adults were fed on 3% sucrose for the first 3–4 days before blood feeding.

Female mosquitoes of the same age and size were fed *at libitum* for 15 min using an artificial blood feeder in which bovine blood meal, supplemented with ATP (5 mM), was added to a parafilm-covered glass vessel. Feeding stations were maintained at 37 °C by a circulating water bath. Individual females fed on 3% sucrose were used as control. To assure that mosquitoes consume the same amount of meal, immediately after feeding each female was examined under microscope, and placed individually in a plastic scintillation vial (covered with a nylon mesh and secured with rubber bands) with access to water. At different times after feeding, the insects were removed from the vials. The excreta of each female were collected by washing the vial with 100 μL of water. The suspension was mixed and centrifuged twice at 14,000 × *g* for 10 min, and the supernatant was filtered through a Microcon centrifugal filter device, YM-30 from Millipore (Billerica, MA, USA). For the identification of Arg, 5 μL of filtrate was mixed with 2.5 μL of 1 mM $^{15}N_2$-Arg. Samples were dried using a vacuum centrifuge and then derivatized to isobutyl esters as indicated above.

Collision-induced dissociation experiments

Collision-induced dissociation (CID) experiments were performed on an Applied Biosystem 4000 QTRAP mass spectrometer (Foster City, CA, USA) with an ESI source operated in the positive ion mode. MS^2 experiments were performed using the product ion scan. MS^3 was performed by optimizing the declustering potential for a fragment of interest scanned in Q1. Once the first fragmentation in the source is optimized, it can be isolated in Q1, fragmented in q2 and the products scanned in Q3 (a linear trap used in quadruple mode). Standards and samples were dissolved in a solution of H_2O/MeOH (30:70, v/v) containing 0.1% formic acid to reach a concentration of 2.5 μM. The solutions were then electrosprayed into the mass spectrometer with a flow rate of approximately 7.0 μL/min. The applied electrospray voltage was 4.8 kV, and the skimmer was at ground potential. The ESI capillary temperature was maintained at 150 °C. Other source and ion optics parameters are stated with each spectrum. Nitrogen served as the collision gas with a collision cell pressure of 8 mTorr. Monoisotopic precursor ions were selected as precursors at unit mass resolution in order to avoid ambiguities from isotope contributions.

Statistical analysis

One way analysis of variance followed by Dunnett's Multiple Comparison Test were used. Data are presented as mean ± standard error of five independent biological samples. A *p*-value less than 0.05 was considered to reflect a statistically significant difference between groups of data. All the statistical analyses were carried out using GraphPad Prism 4.0 Software (GraphPad Prism 4.0 Software, Inc., San Diego, CA).

Results and discussion

In order to facilitate the description and discussion of the data, the fragmentation spectra obtained from derivatized and underivatized Arg (Fig. 1 and Fig. 2) will be first discussed with the proposed fragmentation pathways of the isobutyl ester of Arg presented in Scheme 1. It was elucidated by MS^3 utilizing in-source-CID, and performing a product ion scan on fragments of interest (Fig. 3, Fig. 4, SI Fig. 1, SI Fig. 2). Later, the quantification of Arg by MRM will be shown and discussed.

Fragmentation spectra and proposed fragmentation pathways of the isobutyl ester of arginine

To investigate the fragmentation mechanism of the isobutyl ester of Arg, both unlabeled and $^{15}N_2$-Arg (labeled at the guanidino

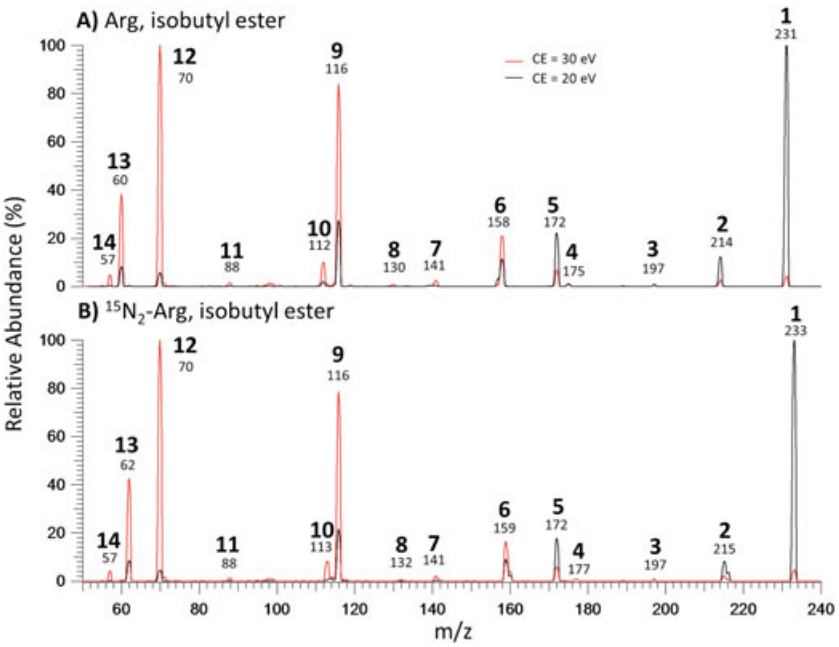

Figure 1. MS/MS spectra of unlabeled and labeled isobutyl ester of Arg **(1)**: A) $[Arg + H]^+$ (*m/z* 231). B) $[^{15}N_2$-Arg (labeled at the guanidino group) $+ H]^+$ (*m/z* 233). The declustering potential (DP) was 72 V, the collision energy (CE) was 20 eV (black spectrum) and 30 eV (red spectrum), entrance potential (EP) was 8 and cell exit potential (CXP) was 9. Signal was acquired for 2 min, and each spectrum was scanned between *m/z* 40 and 300 and at 0.5 s/scan. Structures assigned to the labels are described in Scheme 1 and discussed in the text.

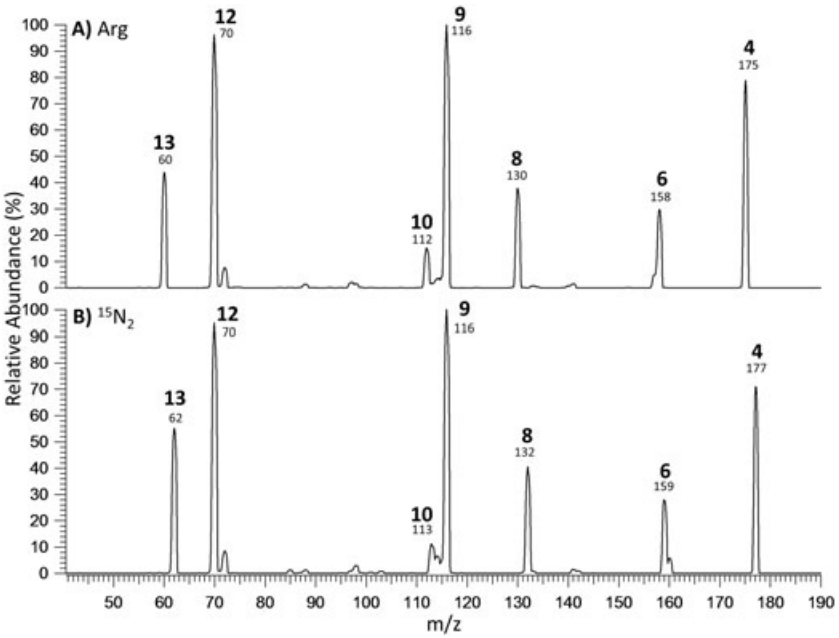

Figure 2. MS/MS spectra of unlabeled and labeled Arg **(4)**: A) $[Arg + H]^+$ (*m/z* 175). B) $[^{15}N_2$-Arg (labeled at guanidino group) $+ H]^+$ (*m/z* 177). DP: 20 eV, CE: 21 eV, EP: 10, CXP: 15. Signal was acquired for 2 minutes and each spectrum was scanned between *m/z* 40 and 300 and at 0.5 s/scan. Structures assigned to the labels are described in Scheme 1 and discussed in the text.

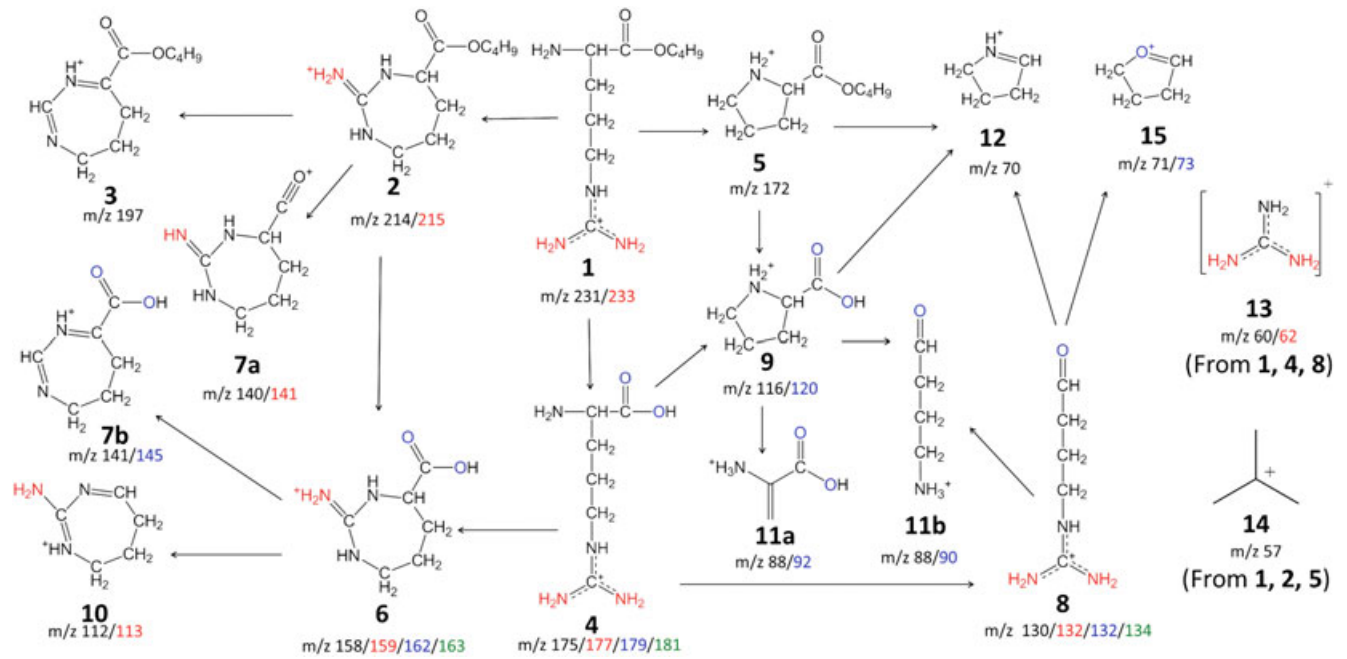

Scheme 1. Proposed fragmentation pathways for the isobutyl ester of Arg. The labeled atoms and *m/z* shown in red were ^{15}N labeled, the labeled atoms and *m/z* shown in blue were ^{18}O labeled, the labeled *m/z* shown in green were ^{15}N-^{18}O labeled. The masses are reported as unlabeled/labeled.

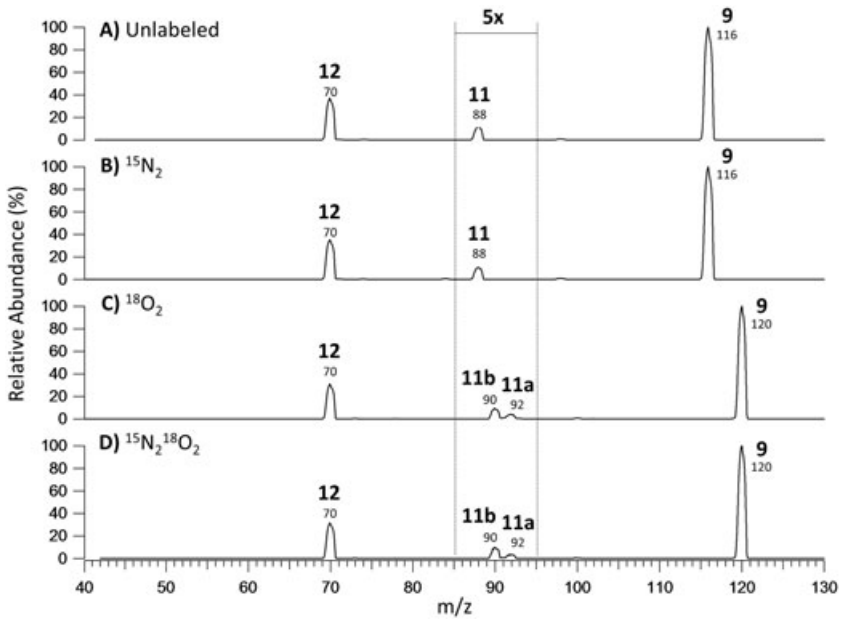

Figure 3. MS^3 of the product ion **(9)** obtained from precursor ion **(4)**. Q1 selection of: A) *m/z* 116 from $[Arg + H]^+$ (*m/z* 175). B) *m/z* 116 from $[^{15}N_2$-Arg (labeled at the guanidino group) $+ H]^+$ (*m/z* 177). C) *m/z* 120 from $[^{18}O_2$-Arg $+ H]^+$ (*m/z* 179). D) *m/z* 120 from $[^{15}N_2$-$^{18}O_2$-Arg $+ H]^+$ (*m/z* 181). DP: 95 eV, CE: 13 eV, EP: 10 and CXP: 15. The region between *m/z* 85–95 was magnified five fold (5x). Signal was acquired for 5 min, and each spectrum was scanned between *m/z* 40 and 300 and at 0.5 s/scan. Structures assigned to the labels are described in Scheme 1 and discussed in the text.

group) were derivatized. The product ion spectra of the unlabeled and $^{15}N_2$-Arg isobutyl esters **(1)** are observed at *m/z* 231 and 233 are presented in Fig. 1A and B, respectively. The proposed fragmentation pathways are summarized in Scheme 1, which shows a total of 15 numbered fragments. The underivatized Arg **(4)** fragment is produced from the isobutyl ester **(1)** by a McLafferty-like rearrangement of the ester and appears at *m/z* 175/177 (Fig. 1A and B, respectively). The remaining many fragments **(2), (3), (5–15)** can then be organized into two major pathways; the first is the S_N1 attack by the lone electron pair of the α-N on the guanidino-C of **(1)** and **(4)** to form a seven member ring, giving **(2)**, **(6)** and subsequent fragments **(3), (7)** and **(10)**. The other is the S_N1 attack by the α-N on the δ-C of **(1)** and **(4)** with subsequent loss of neutral guanidino to form proline species, giving **(5)**, **(9)** and subsequent fragments **(11), (12)** and **(15)**. The guanidinium ion **(13)** seen at *m/z* 60/62 can be obtained for the precursors **(1** and **4)**, as well as from **(8)**, whereas the isobutyl cation **(14)** observed at *m/z* 57 can be

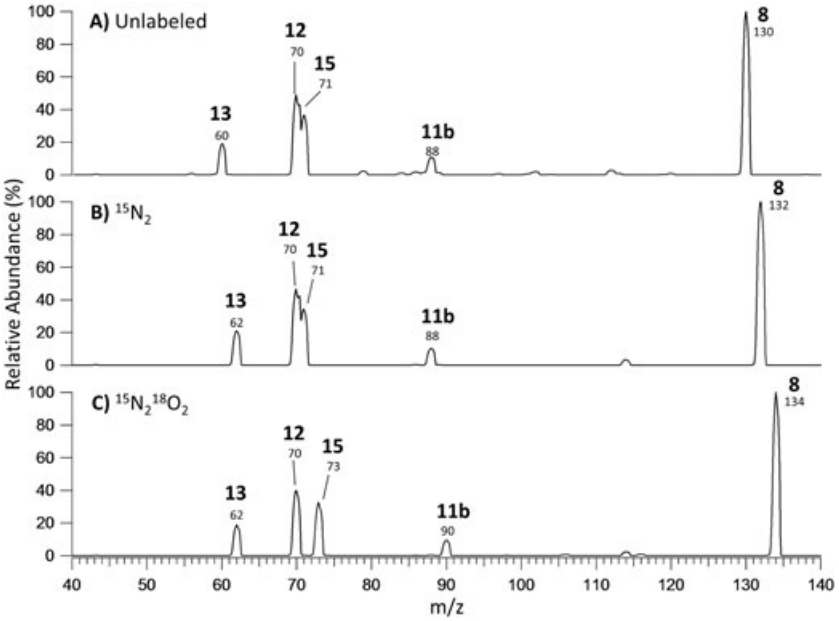

Figure 4. MS^3 of the product ion **(8)** obtained from precursor ion **(4)**. Q1 selection of: A) *m/z* 130 from $[Arg + H]^+$ (*m/z* 175). B) *m/z* 132 from $[^{15}N_2$-Arg (labeled at the guanidino group) $+ H]^+$ (*m/z* 177). C) *m/z* 134 from $[^{15}N_2$-$^{18}O_2$-Arg $+ H]^+$ (*m/z* 181). DP: 95 eV, CE: 13 eV, EP: 10 and CXP: 17. Signal was acquired for 5 min, and each spectrum was scanned between *m/z* 40 and 300 and at 0.5 s/scan. Structures assigned to the labels are described in Scheme 1 and discussed in the text.

formed from the ester precursor **(1)**, as well as from **(2)** and **(5)**, as will be discussed below.

Products resulting from the formation of a seven membered ring

Both the isobutyl ester of Arg **(1)** and Arg free acid **(4)** undergo cyclization through a S_N1 attack by the lone electron pair of the α-N on the guanidino-C. In the fragmentation spectrum of the isobutyl ester, this reaction results in the cyclic structure **(2)** as seen at *m/z* 214 and 215 in Fig. 1A and 1B, respectively. These mass shifts are expected since one ^{15}N label is lost from the guanidino moiety as ammonia. In the fragmentation spectrum of Arg *m/z* 175 **(4)**, the cyclic structure **(6)** appears at *m/z* 158/159 (Fig. 2 A and B) and has been reported previously.[28–30] The cyclic structure **(6)** can originate from a combination of the aforementioned cyclization from **(4)** and the McLafferty-like rearrangement of the ester from **(2)** (Scheme 1), but the order of the reactions is uncertain. The MS^3 of the product ion **(2)** obtained from precursor ion **(1)** (data not shown) indicates that **(6)** can originate from **(2)**. However, it has not been determined if the precursor **(2)** or **(4)** or a combination of both is the sole precursor of **(6)**. The small peak at *m/z* 197 **(3)** seen in the fragmentation spectrum of *m/z* 231/233 **(1)** in Fig. 1 is also observed in the MS^3 fragmentation of both unlabeled and labeled product ions *m/z* 214/215 **(2)** from the precursor isobutyl ester of Arg **(1)**, indicating a cyclic structure resulting from the further loss of the last labeled nitrogen. The formic acid loss of *m/z* 158 **(6)** gives the cyclic structure **(10)** at *m/z* 112/113. Although **(10)** could also result from a butylene loss and further formic acid loss from **(1)**, this is not likely as **(10)** was not seen from **(2)**. The peak at *m/z* 141 **(7)** in Fig. 1 could correspond to an isobutanol loss from the labeled ester **(2)** to give **(7a)** or a neutral loss of NH_3 from the free acid **(4)** to give **(7b)**, which is observed in the MS^3 of the product ion **(2)** obtained from precursor ion **(1)**. In the MS^3 of the product ion **(6)** obtained from precursor ion **(4)** (SI Fig. 1 A and B), no shift occurs for the unlabeled and $^{15}N_2$ labeled compounds. However, a clear 4 Da shift is seen from *m/z* 141 to 145 for the unlabeled and $^{18}O_2$ labeled spectra (SI Fig. 1 A, C and D), regardless of $^{15}N_2$ labeling. Thus, the most likely structure for the peak at *m/z* 141 from **(6)** is **(7a)** because both $^{15}N_2$ labels are lost.

Products resulting from the formation of proline

The S_N1 attack on the δ-C and subsequent loss of neutral guanidino will form Pro at *m/z* 116 **(9)** from Arg **(4)** and the isobutyl ester of Pro at *m/z* 172 **(5)** from the isobutyl ester of Arg **(1)**. This cyclization to form Pro has been reported previously [27,28,30] for Arg, but not for the isobutyl ester although the presence of the ester would not be expected to alter the guanidino loss. Both **(5)** and **(9)** can be found in the product ion spectrum of **(1)** at *m/z* 172 and 116 (Fig. 1A and 1B), respectively, without the $^{15}N_2$ labels that are lost with the neutral guanidino. We also confirmed that Pro **(9)** comes from its isobutyl ester **(5)** by fragmenting **(5)** from **(1)** (SI Fig. 2). The formation of Pro from Arg has implications for the analysis of Pro from complex samples and shotgun proteomics sequencing, because if enough energy is deposited into an N-terminal Arg species in the ion source, it can be cyclized to form Pro, which gives a characteristic peak.[26–30] In an infusion amino acid analysis, it would be possible for Pro to be formed in the source from Arg, an interference in proline analysis which could be overcome by adding chromatography to the front end of the analysis.

Another characteristic fragment of Arg found in the fragmentation spectrum of its isobutyl ester **(1)** (Fig. 1) is the α-NH_3 and CO loss that results in 4-guanidyl-1-butanal **(8)** at *m/z* 130/132. Our data indicate that guanidyl moiety remains intact via the shift from 130 to 132 in the $^{15}N_2$-Arg (Fig. 1). The α-NH_3 and CO loss has been shown previously in the literature using labeled α-^{15}N-Arg.[30]

The structure for the peak at *m/z* 88 was proposed to be 4-amino-1-butanal **(11b)**,[30] as it has been shown to be derived from underivatized Arg and its fragment **(8)** at *m/z* 130 (Fig. 2). A peak at *m/z* 88 also exists in the fragmentation spectrum of

Journal of MASS SPECTROMETRY

Pro (data not shown) and in the MS^3 of the product ion **(9)** obtained from precursor ion 175/177 (4) (Fig. 3, A–B). We hypothesize that there could be a different chemical species for *m/z* 88 peak because the formation of **(11b)** is less likely from Pro **(9)** because the pathway to form **(8)** from Pro **(9)** would require a CO loss, which is less feasible without the electronic interactions provided from the guanidino group.[30] Because **(8)** is not a prominent product of the isobutyl ester **(1)** (Fig. 1A), the peak at *m/z* 88 in the isobutyl ester spectrum is most likely derived directly from Pro, which could result in a structure such as **(11a)**. In order to investigate this possible structure, Arg was labeled with ^{18}O. The fragmentation of $^{18}O_2$-Pro **(9)** from *m/z* 179 $^{18}O_2$-Arg and *m/z* 181 $^{15}N_2^{18}O_2$-Arg (Fig. 3 C-D) gives two peaks shifted from *m/z* 88: one at *m/z* 90 and another at *m/z* 92, clearly showing that one product retains both oxygen atoms **(11a)**, and another retains one oxygen **(11b)**. As expected, the fragmentation of *m/z* 134 $^{15}N_2^{18}O_2$-Arg **(8)** from *m/z* 181 **(4)** shows only the peak at *m/z* 90 (Fig. 4C) shifted from *m/z* 88 (Fig. 4 A-B) supporting the 4-amino-1-butanal structure **(11b)**. Although **(11b)** is the only *m/z* 88 fragment originating from **(8)**, two different fragments with *m/z* 88, **(11a)** and **(11b)**, originate from **(9)**.

A product common to **(1)**, **(4)** and **(8)** is the guanidinium ion **(13)** at *m/z* 60/62. It is seen in the product ion spectra of derivatized Arg (Fig. 1A), underivatized Arg (Fig. 2) and the fragmentation of **(8)** formed from unlabeled Arg (*m/z* 175), $^{15}N_2$ labeled Arg (*m/z* 177) or $^{15}N_2^{18}O_2$ labeled Arg (*m/z* 179) **(4)** (Fig. 4). The isobutyl cation **(14)** observed at *m/z* 57 can be formed from the precursor **(1)**, as well as from the ammonia loss products **(2)** and **(5)**, as seen in the product ion spectra of derivatized Arg (Fig. 1), and in MS^3 of the isobutyl ester of proline **(5)** isolated from the isobutyl ester of Arg **(1)** (SI Fig. 2).

One of the most prominent fragment ions in both the Arg **(4)** and isobutyl ester Arg **(1)** fragmentation spectra is the 1-pyrroline **(12)** at *m/z* 70. This can result from one of two processes. The first process is the formic acid loss from Pro **(9)** or ester rearrangement and further formic acid loss from isobutyl ester of Pro **(5)**. The second minor process is the cyclization resulting from the ε-N attack on the aldehyde of **(8)** with subsequent loss of water and carbodiimide. The pathway from **(8)**, however, likely does not contribute significantly to the population of *m/z* 70 **(12)** as the level of **(8)** formed from the isobutyl ester (Fig. 1A) is small. This agrees with previous experiments on underivatized Arg [30], which have shown that the α-NH_3 is the primary constituent of the 1-pyrroline. The structure at *m/z* 71 **(15)** contains oxygen, and it originates from **(8)**. The oxygen labeling shows that the peak at *m/z* 71, which shifts by 2 Da for $^{18}O_2$ labeled precursor, is indeed a cyclic oxonium ion structure **(15)** (Fig. 4C).

Quantification of arginine by MRM experiments

Based on the fragmentation pathways of isobutyl ester of Arg, two different transitions were used for accurate Arg quantification by tandem mass spectrometry (Table 1). The (231 *m/z*) → (70 *m/z*) and (231 *m/z*) → (116 *m/z*) transitions were chosen as they gave the strongest signals. As indicated in the Experimental Section, the mosquito excreta were collected before and after feeding them with a blood meal. After sample preparation, Arg in the excreta was quantified by MRM at 30 eV in a triple quadrupole Qtrap instrument. The data were processed as indicated previously for other compounds.[6–10]

The analytical characteristics of the method are described in Table 2. The recovery of the sample after filtration was greater than 85% for all standards between 0.01 and 1 mM. The linear range of the method was determined to be between 2.7 μM and 667 μM. Limit of detection was determined to be 0.5 μM taken as 3:1 ratio of signal to background signal.

Table 1. *m/z* of precursor ions selected, mass of neutrals lost and MRM transitions

Amino acid	Precursor ion	Neutral loss	Precursor ion/ Fragment ion pair
Isobutyl ester of Arginine	231	161	231 → 70
		115	231 → 116
Isobutyl ester of [$^{15}N_2$]-Arginine	233	163	233 → 70
		117	233 → 116

The quantification of arginine can be performed by MRM using [$^{15}N_2$]-Arginine as an internal standard

Table 2. Analytical characterization of arginine quantification method

Recovery after filtration			Standard Curve	
Arg (mM)	**Recovery (%)**	**Standard Deviation**	**Linear Range (μM)**	2.7 to 667
1	90.0	5.6	**R^2**	0.9911
0.1	85.4	2.1	**Slope**	0.8648
0.01	96.4	4.9	**Y intercept**	2.1933
			Lower limit detection (μM)	0.5

The analysis was performed in triplicate

In Fig. 5, identification and time course quantification of Arg in the excreta of individual female mosquitoes is shown. As expected, Arg is not present in the sugar-fed female excreta (data not shown), and only a very small amount is observed in the blood-fed female excreta at 1 and 6 h after feeding a blood meal. At 12 h, the Arg concentration reaches values of approximately 20 nmol/female mosquito. This value increases significantly during the time course investigated, reaching the highest levels between 36 and 48 h (about 60 nmol/female) and remains constant (no further excretion) through the end of the time

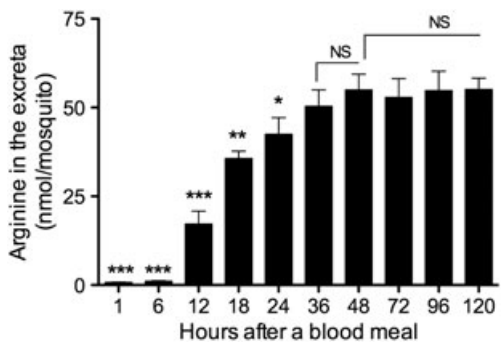

Figure 5. Concentrations of Arg in *A. aegypti* female excreta. Female mosquitoes were fed on 3% sucrose or a bovine blood meal, and the excreta of individual females were analyzed before a blood meal (data not shown) and at 1, 6, 12, 18, 24, 36, 48, 72, 96 and 120 h after feeding a blood meal. Data are presented as mean ± standard error of five independent samples; NS: not significant; *$p < 0.05$, **$p < 0.01$, ***$p < 0.00001$ (when compared with 48 h by analysis of variance).

course (120 h after a blood meal). These data are well correlated with the periods of intense blood meal digestion and maximal excretion of nitrogen compounds in the blood-fed females.[5,8,11]

Uric acid, urea and ammonia are some of the main nitrogen wastes excreted in *A. aegypti* females. The ratio of nitrogen excreted as urea *versus* the nitrogen excreted as uric acid in mosquito excreta at 72 h after a blood meal feeding is about 1:3, whereas the ratio between nitrogen excreted as urea *versus* nitrogen excreted as ammonia is about 1:1.[11] Notably, the Arg concentration reported here at 24 h is comparable to the previously reported urea concentration excreted at 24 h by blood-fed *A. aegypti* females.[8] Dietary Arg in mosquitoes can follow diverse metabolic pathways, i.e. it can be utilized for protein synthesis, hydrolyzed into ornithine and urea, metabolized into nitric oxide or excreted directly without any modification during the digestion of a blood meal. Indeed, the results reported here show that Arg excretion contributes to the elimination of nitrogen excess in blood-fed mosquitoes. This seems to be a very important strategy of nitrogen disposal considering that mosquito females ingest large amounts of protein with a blood meal. In fact, an *A. aegypti* female can ingest as much as her own weight or more in a blood meal. However, only a small percentage of the nitrogen ingested is utilized to maintain different metabolic processes such as energy and egg production; the excess of the nitrogen ingested is excreted efficiently. A better understanding of the mechanisms involved in nitrogen metabolism in mosquitoes may facilitate the design of new strategies for controlling mosquito populations.

The quantification of Arg by tandem mass spectrometry provides a rapid, sensitive and accurate method to further investigate the metabolic regulation of nitrogen waste in individual *A. aegypti* mosquitoes. This approach can also be applied to quantify Arg in other mosquito species, as well as other invertebrates, whose small size limits the use of more conventional biochemical techniques.

Acknowledgements

The authors thank Dr. Shai Dagan for helpful suggestions and critical revision of this manuscript and Dr. George Tsaprailis for allowing us the use of the AB/SCIEX 4000 QTRAP mass spectrometer at the Arizona Proteomics Consortium at The University of Arizona. The AB/SCIEX 4000 QTRAP mass spectrometer was provided by NIH/NCRR Grant 1S10RR022384-01. This work was financially supported by National Institutes of Health Grant R01AI088092 (to PYS).

Supporting information

Supporting information may be found in the online version of this article.

References

[1] K. R. Matthews. Controlling and coordinating development in vector-transmitted parasites. *Science* **2011**, *332*, 421–421.
[2] S. Sim, J. L. Ramirez, G. Dimopoulos. Molecular discrimination of mosquito vectors and their pathogens. *Expert Rev. Mol. Diagn.* **2009**, *9*, 757–765.
[3] S. C. Weaver, W. K. Reisen. Present and future arboviral threats. *Antiviral Res.* **2010**, *85*, 328–345.
[4] P. Y. Scaraffia, M. A. Wells. Proline can be utilized as an energy substrate during flight of *Aedes aegypti* females. *J. Insect Physiol.* **2003**, *49*, 591–601.
[5] P. Y. Scaraffia, J. Isoe, A. Murillo, M. A. Wells. Ammonia metabolism in *Aedes aegypti*. *Insect Biochem. Mol. Biol.* **2005**, *35*, 491–503.
[6] Q. Zhang, V. Wysocki, P. Scaraffia, M. Wells. Fragmentation pathway for glutamine identification: Loss of 73 da from dimethylformamidine glutamine isobutyl ester. *J. Am. Soc. Mass Spectrom.* **2005**, *16*, 1192–1203.
[7] P. Y. Scaraffia, Q. Zhang, V. H. Wysocki, J. Isoe, M. A. Wells. Analysis of whole body ammonia metabolism in *Aedes aegypti* using [^{15}N]-labeled compounds and mass spectrometry. *Insect Biochem. Mol. Biol.* **2006**, *36*, 614–622.
[8] P. Y. Scaraffia, G. Tan, J. Isoe, V. H. Wysocki, M. A. Wells, R. L. Miesfeld. Discovery of an alternate metabolic pathway for urea synthesis in adult *Aedes aegypti* mosquitoes. *Proc. Nat. Acad. Sci.* **2008**, *105*, 518–523.
[9] P. Y. Scaraffia, Q. Zhang, K. Thorson, V. H. Wysocki, R. L. Miesfeld. Differential ammonia metabolism in *Aedes aegypti* fat body and midgut tissues. *J. Insect Physiol.* **2010**, *56*, 1040–1049.
[10] W. Jiang, V. H. Wysocki, E. D. Dodds, R. L. Miesfeld, P. Y. Scaraffia. Differentiation and quantification of C1 and C2 ^{13}C-labeled glucose by tandem mass spectrometry. *Anal. Biochem.* **2010**, *404*, 40–44.
[11] P. von Dungern, H. Briegel. Enzymatic analysis of uricotelic protein catabolism in the mosquito *Aedes aegypti*. *J. Insect Physiol.* **2001**, *47*, 73–82.
[12] E. M. Zdobnov, C. von Mering, I. Letunic, D. Torrents, M. Suyama, R. R. Copley, G. K. Christophides, D. Thomasova, R. A. Holt, G. M. Subramanian, H. M. Mueller, G. Dimopoulos, J. H. Law, M. A. Wells, E. Birney, R. Charlab, A. L. Halpern, E. Kokoza, C. L. Kraft, Z. W. Lai, S. Lewis, C. Louis, C. Barillas-Mury, D. Nusskern, G. M. Rubin, S. L. Salzberg, G. G. Sutton, P. Topalis, R. Wides, P. Wincker, M. Yandell, F. H. Collins, J. Ribeiro, W. M. Gelbart, F. C. Kafatos, P. Bork. Comparative genome and proteome analysis of *Anopheles gambiae* and *Drosophila melanogaster*. *Science* **2002**, *298*, 149–159.
[13] B. Zhu, D. Bush, G. A. Doss, S. Vincent, R. B. Franklin, S. Y. Xu. Characterization of 1 '-hydroxymidazolam glucuronidation in human liver microsomes. *Drug Metab. Dispos.* **2008**, *36*, 331–338.
[14] J. E. Adaway, B. G. Keevil. Therapeutic drug monitoring and LC–MS/MS. *J. Chromatogr. B* **2012**, *883–884*, 33–49.
[15] Y. Xiang, J. M. Koomen. Evaluation of direct infusion-multiple reaction monitoring mass spectrometry for quantification of heat shock proteins. *Anal. Chem.* **2012**, *84*, 1981–1986.
[16] R. Manfred. LC–MS/MS for protein and peptide quantification in clinical chemistry. *J. Chromatogr. B* **2012**, *883–884*, 59–67.
[17] S. Stadler, K. Gempel, I. Bieger, B. F. Pontz, K. D. Gerbitz, M. F. Bauer, S. Hofmann. Detection of neonatal argininosuccinate lyase deficiency by serum tandem mass spectrometry. *J. Inherit. Metab. Dis.* **2001**, *24*, 370–378.
[18] D. H. Chace, T. A. Kalas, E. W. Naylor. The application of tandem mass spectrometry to neonatal screening for inherited disorders of intermediary metabolism. *Annu. Rev. Genom. Hum. Genetics* **2002**, *3*, 17–45.
[19] D. H. Chace, T. A. Kalas, E. W. Naylor. Use of tandem mass spectrometry for multianalyte screening of dried blood specimens from newborns. *Clin. Chem.* **2003**, *49*, 1797–1817.
[20] D. H. Chace. Mass spectrometry in the clinical laboratory. *Chem. Rev.* **2001**, *101*, 445–477.
[21] D. H. Chace, D. S. Millington, N. Terada, S. G. Kahler, C. R. Roe, L. F. Hofman. Rapid diagnosis of phenylketonuria by quantitative analysis for phenylalanine and tyrosine in neonatal blood spots by tandem mass spectrometry. *Clin. Chem.* **1993**, *39*, 66–71.
[22] D. H. Chace, S. L. Hillman, D. S. Millington, S. G. Kahler, C. R. Roe, E. W. Naylor. Rapid diagnosis of maple syrup urine disease in blood spots from newborns by tandem mass spectrometry. *Clin. Chem.* **1995**, *41*, 62–68.
[23] D. H. Chace, S. L. Hillman, D. S. Millington, S. G. Kahler, B. W. Adam, H. L. Levy. Rapid diagnosis of homocystinuria and other hypermethioninemias from newborns' blood spots by tandem mass spectrometry. *Clin. Chem.* **1996**, *42*, 349–355.
[24] A. A. Reilly, R. Bellisario, K. A. Pass. Multivariate discrimination for phenylketonuria (PKU) and non-PKU hyperphenylalaninemia after analysis of newborns' dried blood-spot specimens for six amino acids by ion-exchange chromatography. *Clin. Chem.* **1998**, *44*, 317–326.
[25] M.-U. Trinh, J. Blake, J. R. Harrison, R. Gerace, E. Ranieri, J. M. Fletcher, D. W. Johnson. Quantification of glutamine in dried blood spots and plasma by tandem mass spectrometry for the biochemical diagnosis and monitoring of ornithine transcarbamylase deficiency. *Clin. Chem.* **2003**, *49*, 681–684.

[26] B. J. Bythell, I. N. P. Csonka, S. N. Suhai, D. F. Barofsky, B. Paizs. Gas-phase structure and fragmentation pathways of singly protonated peptides with N-terminal Arginine. *J. Phys. Chem. B* **2010**, *114*, 15092–15105.
[27] I. P. Csonka, B. Paizs, S. Suhai. Modeling of the gas-phase ion chemistry of protonated arginine. *J. Mass Spectrom.* **2004**, *39*, 1025–1035.
[28] N. N. Dookeran, T. Yalcin, A. G. Harrison. Fragmentation reactions of protonated α-amino acids. *J. Mass Spectrom.* **1996**, *31*, 500–508.
[29] M. Forbes, R. Jockusch, A. Young, A. Harrison. Fragmentation of protonated dipeptides containing arginine. Effect of activation method. *J. Am. Soc. Mass Spectrom.* **2007**, *18*, 1959–1966.
[30] P. Y. I. Shek, J. Zhao, Y. Ke, K. W. M. Siu, A. C. Hopkinson. Fragmentations of protonated arginine, lysine and their methylated derivatives: Concomitant losses of carbon monoxide or carbon dioxide and an amine. *J. Phys. Chem. A*, **2005**, *110*, 8282–8296.
[31] R. C. Murphy, K. L. Clay. Synthesis and back exchange of ^{18}O labeled amino acids for use as internal standards with mass spectrometry. *Biol. Mass Spectrom.* **1979**, *6*, 309–314.

